Thin Solid Films, *191* (1990) 255–273

PROPERTIES OF MAGNETRON-DEPOSITED POLYCRYSTALLINE TiN LAYERS

J. STANISLAV
Scientific Base of Electrical Heat Equipment Plants, Liberec (Czechoslovakia)
J. SIKAC
State Research Institute of Material Protection, Prague (Czechoslovakia)
M. CERMAK
State Research Institute of Materials, Prague (Czechoslovakia)
(Received June 14, 1989; revised December 18, 1989; accepted February 13, 1990)

Polycrystalline TiN_x layers were magnetron sputtered on substrates of high speed steel, sintered carbide and low carbon steel in an Ar–N_2 atmosphere with various N_2 partial pressures and bias voltages, the deposition rate being from 0.5 μm min^{-1} (metallic mode) to 0.1 μm min^{-1} (reactive mode). The stoichiometry of the layers was evaluated on the basis of thermogravimetric analysis of separated coatings, Auger electron spectroscopy investigation and X-ray powder patterns. The relationship between the X-ray powder diffractograms of coatings on a substrate and separated coatings allowed the role of the thermally based stress in the coatings to be estimated. Maximum values of the compressive stresses were found at biases of -200 to -250 V; for $U_B > -60$ V tensile stresses were observed. The colour coordinates exhibited a strong dependence on N_2 flow rate with an apparent threshold at 35 standard cm^3 min^{-1}, which corresponds to the stoichiometric compound. An increase in the bias voltage leads to an increasing yellow and red tint of the coating. Drilling tests revealed the highest durability for slightly super-stoichiometric coatings. The optimum bias was found to be -100 V, because of the very low or zero internal stress in the TiN_x layer.

1. INTRODUCTION

The magnetron deposition of thin polycrystalline TiN layers produces very good results in practice for improving the useful characteristics of cutting tools and machine parts. However, the application of this method in practice involves certain problems, which are associated with a remarkable dependence of certain TiN properties on the deposition parameters.

In the present work, conclusions are drawn from an investigation of certain important characteristics of magnetron-deposited TiN layers carried out at the Scientific and Research Base of ZEZ Liberec. The purpose of these investigations was to check the effects of particular deposition parameters on basic TiN characteristics and to optimize them with respect to the useful properties.

0040-6090/90/$3.50

2. EXPERIMENTAL DETAILS

2.1. Sample material

Three basic types of samples were used for the experiments, depending on the measurements to be made. The samples for the evaluation of the thickness of the layers, microhardness, adhesion and colour coordinates were made of the high speed steel (HSS) Poldi 19830 with a composition of 0.85 C, 4.2 Gr, 6.25 W and 1.85 V, and size of 24 mm × 4 mm. The samples were thermally treated to 65 ± 1 HRC and their surfaces were polished on one side.

For the X-ray evaluation, samples of sintered carbide H1 with a composition 94% WC and 6% Co were employed.

For the chemical analysis, the samples were made of a low carbon steel sheet of size 50 mm × 80 mm × 1 mm.

Drills of diameter 6 mm made of HSS material served as samples for drilling tests.

2.2. The experimental equipment

The TiN_x layers were deposited in a Z 700 device (Leybold AG) between two magnetron cathodes (PK 500) with a target size of 488 mm × 88 mm × 6 mm. The distance between the cathodes was 120 mm, and the sample-to-cathode distance was 60 mm. Titanium (Poldi 45) of purity 99.45% was used for the deposition process.

The Z 700 device has a pump system, consisting of a rotary vacuum pump ($200\,m^3\,h^{-1}$), a Roots pump ($500\,m^3\,h^{-1}$) and three turbomolecular pumps each of capacity $1000\,l\,s^{-1}$.

The base pressure before the process was carried out was 5×10^{-3} Pa and this pressure was kept for all the sample processes.

Process gases were supplied by mass flow rate meters for argon and N_2. In the course of the process, the atmosphere's composition was checked with a PGA 100 mass spectrometer. The total pressure during the processes in reactive as well as non-reactive modes was measured by a Viscovac VM211 vacuometer. The purities of the gases supplied were as follows: argon, 99.997%; N_2, 99.998%.

2.3. The deposition process

The deposition parameters were organized in such a way that it was possible to follow two basic parameters of the TiN_x layer magnetron deposition process, *i.e.* partial pressure p_{N_2} (Pa) of nitrogen and substrate bias U_B (V), and their effects on the characteristics of the TiN_x layers. In the Z 700 device it is possible to apply eight layers to samples with different parameters within one process. Sample series were set up in such a way that only the nitrogen flow rate was varied within one series at a constant U_B value. On the first sample only pure titanium was applied. The layers were deposited on both sides.

Samples were degreased before deposition in alkaline aqueous solutions with subsequent rinsing with water, At the final stage the samples were dried in Freon TDA-35X and Freon TF.

After evacuation of the operating chamber to a pressure of 5×10^{-3} Pa, the samples were sputter cleaned in an argon atmosphere at a pressure $p_T = 1.7$ Pa at a

maximum voltage $U_E = 1700\,V$ for $t_E = 10\,min$. In the course of cleaning, and heating the sample, magnetrons served as a source of the auxiliary ionization of the medium with $I_M = 0.3\,A$.

During deposition the magnetron current I_M was 8.5 A and the power related to the target area P_M was $10\,W\,cm^{-2}$. The total pressure was 1.1 Pa and it was obtained by supplying 200 ml Ar min^{-1}. The nitrogen flow rate within a series of samples was varied as follows: 0, 30, 35, 40, 50, 70, 90 and 120 ml min^{-1}. A total of three sample series was used, treated at bias values $U_B = -100$, -150 or $-200\,V$. The films obtained were 3–5 μm thick.

3. EVALUATION METHODS

3.1. The layer thickness

The layer thickness was measured by the Kalotest method with a ball of diameter 44 mm. The layer thickness was checked on separated deposits by scanning electron microscopy and orientationally also by gravimetric and X-ray diffraction methods.

3.2. The microhardness

The microhardness measurements were carried out with an Epitype 2 instrument by the Hanemann method using a Vicker's indenter at loads $F = 0.01$ and 0.02 kgf. The evaluation of the indentations was performed optically with a magnification of 400×.

3.3. The layer adhesion

The adhesion between the TiN layer and substrate was measured on a Zwick 3312 hardness tester with the help of the scratch test. The load was varied discontinuously, and the sample stage moved with a constant velocity. The scratch was produced by a Rockwell indenter and the loss of adhesion was evaluated by an optical method.

3.4. The chemical composition of TiN layers

The chemical analysis of samples was performed by Auger microscopy with a high resolution Auger electron spectroscopy (AES) instrument (Varian, U.K.) at Dr. Sundgren's laboratory at the University of Linköping and also by a chemical method.

The Auger spectra were acquired in the range 30–530 eV with a rate of 100 eV min^{-1}. The spectra were measured after ion etching with Ar^+ ions with an ion gun, at an ion current of 20 μA for 4 min.

The chemical analysis was performed by a gravimetric method on separated coatings. The layers were separated from the substrate in 15% HCl, decanted with water, dried and annealed in a platinum crucible in air at 800 °C and weighed as TiO_2. The complete phase transition of TiN to TiO_2 was checked by the X-ray diffraction method.

3.5. The X-ray phase analysis

The X-ray phase analysis of thin layers was performed on Philips and Siemens

instruments using monochromatic Cu Kα and Co Kα radiation with a continuous 2θ scan (0.25° min^{-1} or 0.125° min^{-1}) in an angular interval including the diffraction lines (111), (200) and (220) of TiN and one or two lines of the substrate. In our case these were the (100) and (101) lines of WC. When powderized samples, which had been applied onto silver foil, were evaluated, Ag(111) and Ag(200) reflections were measured.

From the diffractographs obtained, on the one hand maxima of particular diffraction lines were located and, on the other hand, areas of diffraction lines of TiN and substrate were measured by a planimeter.

3.6. The measurement of colour coordinates

The measurement of colour coordinates was carried out on a Gardner spectral colorimeter in the region of visible light from 400 to 700 nm and the colour coordinates were established for normalized D65 illumination. The measurements were carried out on an area of diameter 22 mm with exclusion as well as inclusion of the lustre. The colour was evaluated in the CIEL a^*b^* system.

3.7. The wear tests

Drills of diameter 6 mm were used for wear tests. The tools were made of the HSS material. An FNK 32 milling machine was used for the tests. The parameters of drill testing were $n = 1800\,min^{-1}$, $s = 0.07$ and $0.14\,mm\ rev^{-1}$, drilling depth $h = 18$ mm. A cooling emulsion was used. The tools were tested in 15142 Poldi material (0.45 C, 0.80 Mn, 0.37 Si, 1.2 Cr, 0.3 Mo) refined to 1000 MPa.

4. THE EVALUATION OF EXPERIMENTS

4.1. The deposition rate

The rate of deposition in the course of magnetron application of TiN layers depends on a number of parameters. These are parameters affecting the process of supplying titanium to the cathode and also parameters affecting the transport of particles from the cathode to the substrate and last but not least parameters affecting the condensation of the layer on the base.

The partial pressure of the reactive gas (nitrogen) is one of the most important parameters. The dependence in Fig. 1 shows the typical behaviour of the rate of the deposition as a function of the nitrogen flow rate. A maximum deposition rate was achieved in the metallic mode of material supply for the deposition and this was 0.3–0.5 μm min^{-1}. When the partial pressure of nitrogen is increased stepwise, then reactive products of TiN_x are deposited on the targets at sites with a low magnetic field intensity with a stepwise reduction in the capacity of the target to supply material.

Beyond the transient region the deposition enters the reactive mode, where the deposition rate decreases to as little as 20% of the initial deposition rate and its value is about 0.1 μm min^{-1}.

Target clogging during reactive deposition is also connected with a so-called hysteresis effect in the dependence of the partial pressure on the nitrogen flow rate[1]. This effect is undesirable from the standpoint of the deposition since as well as the

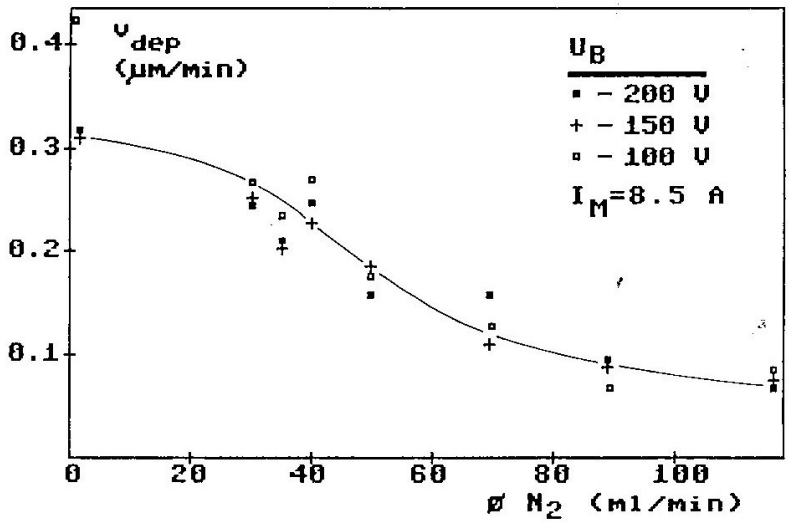

Fig. 1. The dependence of the deposition rate on the nitrogen flow rate for a pair of PK 500 magnetron cathodes.

decrease in deposition rate it also causes the reproducibility of the process to deteriorate. Its removal is dependent to a certain extent on the vacuum system pumping rate[2]. When this pumping rate is higher than a critical value, the hysteresis effect may be completely absent.

4.2. The adhesion of the layer to the base material

The adhesivity of the layer to the base may principally affect the useful characteristics of the layer in the working process. It is affected by a relationship between the substrate and the layer deposited. It has been demonstrated that the coherence on the substrate layer interface affects positively the value of the adhesion force by reducing elastic stresses in the layer[3]. On steel substrates, the adhesion of the layers is affected positively, *e.g.* by a conversion of the oxides Fe_2O_3 and Fe_3O_4 to FeO as speculated in ref. 3 and the occurrence of carbidic particles of the type MC (*e.g.* VC). The structure of these components is B1-NaCl and their lattice parameters are very close to those of TiN. The coherence of the lattice of the layer with these MC particles on the substrate surface makes possible a local epitaxial growth of the layer[4].

Figure 2 shows the dependence of the measured adhesion force on the nitrogen flow rate for three bias values ($U_B = -100$, -150 and -200 V). Minimum adhesion values are achieved at 30–35 ml min^{-1} of nitrogen. This is a region of maximum values of the layer's microhardness and maximum values of elastic stresses in the layer. In the region above 30 ml min^{-1} of nitrogen, the layer consists of only the δ-TiN phase, *i.e.* a phase with a basic B1-NaCl structure. The change in the chemical composition of the layer at this nitrogen flow rate is very small and thus it has no significant effect on the adhesion. There is, however, a marked difference in physical characteristics of the layer. In particular, for higher flow rates of nitrogen the value of the macroscopic stresses in the layer increases and this affects positively the value of the adhesion force. The values of the microstress in the layer and the texture are, however, also altered.

On the basis of the values measured it is impossible to conclude that there is a

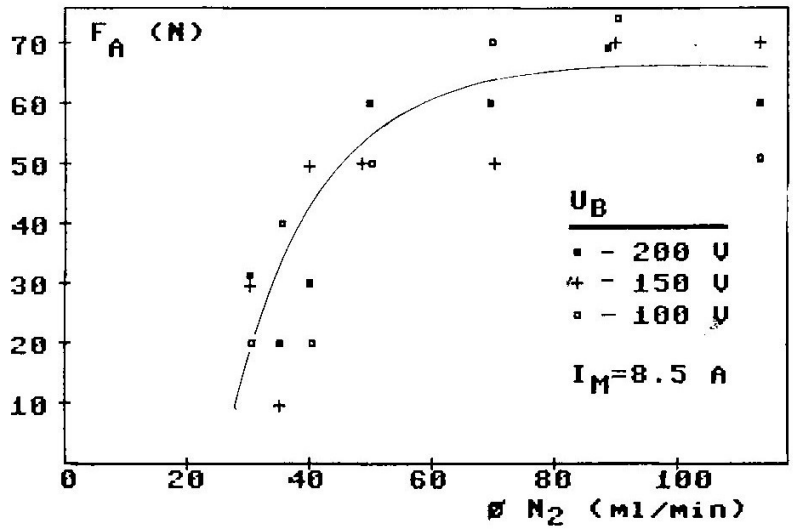

Fig. 2. The dependence of the adhesion force on the nitrogen flow rate for series of samples at $U_B = -100$, and -300 V.

marked dependence of the layer's adhesion on the bias U_B. In particular, this parameter affects positively the growth of the layer from the standpoint of its morphology, its purity etc. With respect to low particle energies, no significant implantation effect may occur.

4.3. The microhardness of the TiN_x layer

The TiN_x layers exhibit high microhardness values. This results from a high contribution of the covalent bond between titanium and nitrogen atoms and a low proportion of the ionic bond.

The microhardness of the TiN layer is strongly dependent on the amount of reactive gas in the operating atmosphere. This dependence is plotted in Fig. 3 for three bias values.

The microhardness of the layer achieves its remarkable maximum in a region of flow rates from 30 to 35 ml min^{-1} of nitrogen and then the layer microhardness decreases with further increases in the amount of nitrogen in the atmosphere.

For nitrogen flow rates of 0–30 ml min^{-1}, the layer formed consists only of α-Ti with a hexagonal lattice, which is stepwise oversaturated with interstitial nitrogen. At a flow rate of 20 ml min^{-1} only the α-Ti phase was found in the layer; however, the layer microhardness was as high as 2000 HV 0.01. For a flow rate of 25 ml min^{-1}, the layer was formed exclusively of the δ-TiN phase. The ε-Ti_2N phase is completely suppressed, which is typical for the magnetron deposition of TiN. The ε-Ti_2N phase is produced only under exceptional deposition conditions[5].

When the material strengths are assumed to be connected with the lattice perfection, then in the region of the microhardness maximum there will also probably be a maximum in the covalent bond contribution. In contrast, with an increasing amount of vacancies, either of nitrogen or those at titanium sites[6], the ionic bond proportion will be increased. The layer microhardness will decrease.

This phenomenon may be observed at nitrogen flow rates above 40 ml min^{-1}. In this region, the layer is already moderately superstoichiometric with N:Ti = 1.05–1.1, probably with vacancies at titanium sites[7]. At flow rates below

30 ml min^{-1} the microhardness decreases again, although much more strongly. The layer is substoichiometric and with decreasing nitrogen content it is even converted to α-Ti. The decrease in the microhardness and development of the substoichiometry are probably significantly affected by a growth of vacancies at nitrogen sites. The growing bias on the substrate moderately increases the layer's microhardness. This phenomenon is connected with an increasing macroscopic stress in the layer; however, it is also connected with a moderate decrease in the stoichiometry as a result of an increased capacity to supply material for deposition, particularly for nitrogen on the substrate.

4.4. The chemical analysis of TiN_x layers with Auger electron spectroscopy

AES was employed to perform the chemical analysis of all the samples of TiN_x layers mentioned. Figure 4 shows a typical spectrum for the TiN layer deposited at a flow rate of 35 ml N_2 min^{-1} and at $U_B = -150$ V. The N:Ti ratio was established according to the method of Dawson[8] from the total height of peaks at 383 and 418 eV. The proportions of carbon, oxygen and argon in the layer were negligible after sputter cleaning for 4 min.

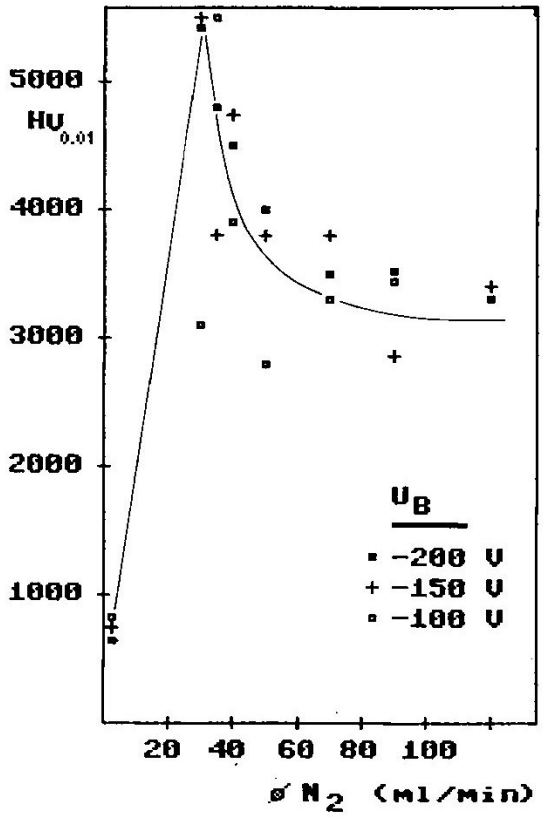

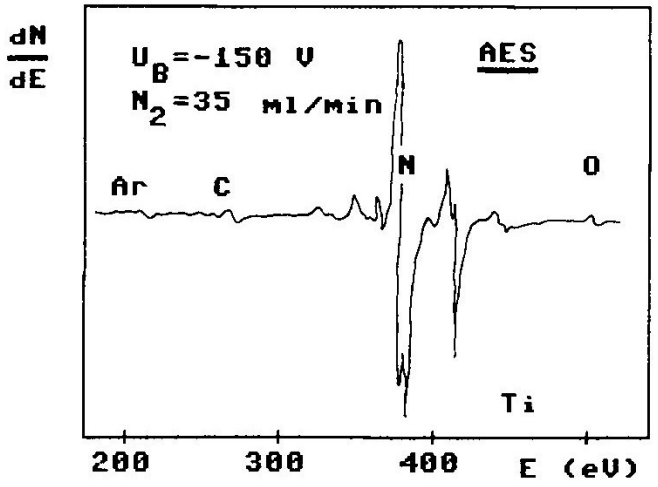

Fig. 3. The dependence of the TiN layer microhardness on the nitrogen flow rate for bias values $U_B = -100$, -150 and -200 V.

Fig. 4. A typical Auger electron spectrum of a TiN_x layer deposited at a nitrogen flow rate of 35 ml min^{-1} and a bias $U_B = -150$ V.

Figure 5 shows the dependence of the stoichiometric ratio $x = [N]/[Ti]$ on the nitrogen flow rate. The dependence is plotted for all three bias values U_B. The stoichiometric ratio is achieved at a nitrogen flow rate of 35–40 ml min^{-1}. The layer

composition is not substantially altered by a further increase in the nitrogen flow rate.

The effect of the bias on the layer's stoichiometry is not remarkable. This effect is most strongly manifested by a change in colour coordinates of the layer.

4.5. The chemical gravimetric analysis of TiN_x layers

The chemical analysis of the layers was performed by a gravimetric method on coatings which were separated from the substrate in 15% HCl with an admixture of hydrogen peroxide. On the basis of the amount of the coating separated, the thickness was calculated orientationally and the coating was annealed in a platinum crucible at 800 °C in air. Decomposition of TiN with its oxidation to TiO_2 occurs according to the scheme

$$2TiN + O_2 \xrightarrow{800\,^\circ C} 2TiO_2 + N_2 \tag{1}$$

After weighing, the titanium content in the original samples was calculated and then the stoichiometric factor x was calculated from the formula

$$x = \frac{M_{Ti}}{M_N}\left(\frac{100}{C_{Ti}} - 1\right) \tag{2}$$

where M_{Ti} and M_N are the atomic masses of titanium and nitrogen respectively, and C_{Ti} (wt.%) is the titanium content obtained.

The resulting dependence of the TiN chemical composition in the nitrogen flow rate is shown in Fig. 6 and it displays a behaviour very similar to that of Fig. 5. With

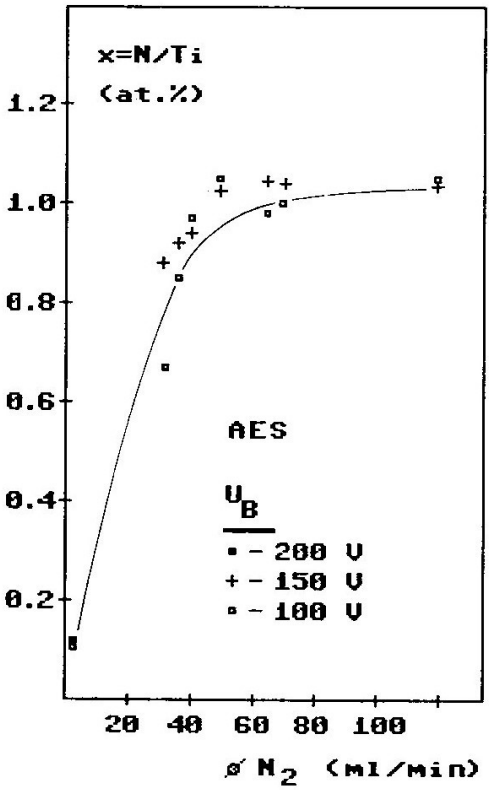

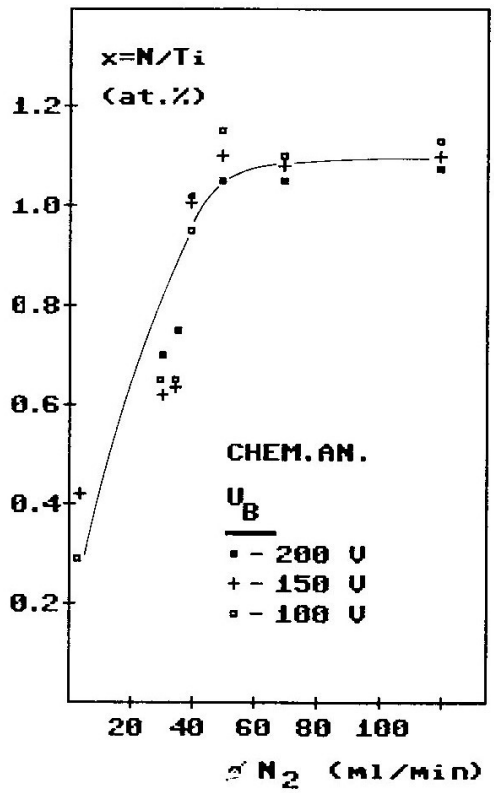

Fig. 5. The dependence of the N:Ti stoichiometric ratio on the nitrogen flow rate evaluated from Auger spectra.

Fig. 6. The dependence of the N:Ti stoichiometric ratio on the nitrogen flow rate evaluated by chemical gravimetric analysis.

respect to the agreement of the results it can be concluded that in certain cases it is possible to use the chemical gravimetric method for establishing the stoichiometry of physically applied TiN_x layers.

4.6. The X-ray phase analysis

4.6.1. The texture evaluation

The magnetron-deposited TiN layers are textured. This means that certain crystallographic planes occur more frequently than others. To proceed further with the calculation of lattice parameters the texture coefficient TK_{hkl} was employed. This coefficient was determined according to the following formula:

$$TK_{hkl} = \frac{(I/R)_{hkl}}{\Sigma_{j=1}^{N}(I/R)_j} \tag{3}$$

where the I (mm^2) are integrated intensities of the diffraction lines used and the R are calculated intensities for a random powder for a system of the planes with indices hkl.

The dependence of the texture coefficient TK_{hkl} on the nitrogen flow rate for a series of samples with a bias $U_B = -150$ V is shown in Fig. 7. The figure shows that in the layer there is a texture in the (111) direction and it reaches its maximum in the nitrogen flow rate interval from 50–60 ml min^{-1}. Figure 8 presents the dependence of the texture coefficient TK_{111} on nitrogen flow rate for all three bias values used. The value of the bias affects strongly the texture and, with its growth, the preferred orientation of the layer in the crystallographic direction (111) is increased. This

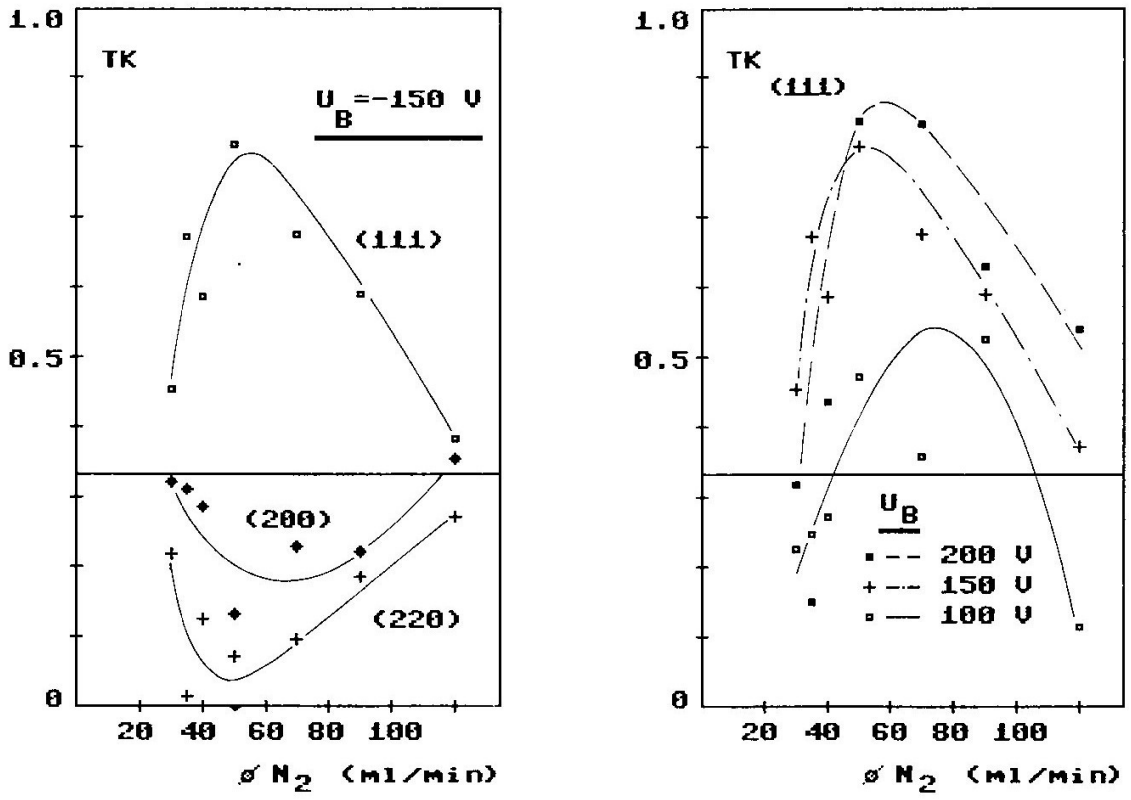

Fig. 7. The dependence of the texture coefficients TK_{111}, TK_{200} and TK_{220} on the nitrogen flow rate.

Fig. 8. The dependence of TK_{111} on the nitrogen flow rate for samples with $U_B = -100$, -150 and -200 V.

phenomenon may be suppressed by increasing the ion current on the substrate as shown in Fig. 9, where the texture of the layer decreases in the (111) direction and the proportion of crystallites oriented in the (200) and (220) directions increases with increasing ion current.

The X-ray analysis of the layers was also performed on samples of separated TiN_x layers. These layers were stripped from the substrate according to the method described in Section 3.4. In these separated layers the texture disappears; all intensities for (111) (200) and (220) directions correspond to those for a random powder.

4.6.2. The evaluation of lattice parameters

On the basis of the particular diffraction lines (111), (200) and (220), values of the lattice parameter were evaluated. Since the representation of particular crystallographic planes is proportional to the texture coefficient according to formula (3), the resulting lattice parameter was calculated as a weighted mean value from the formula

$$a_{TK} = a_{111}TK_{111} + a_{200}TK_{200} + a_{220}TK_{220} \tag{4}$$

The lattice parameter a_{TK} was corrected for the macroscopic stress originating in the layer by the action of differing thermal expansions of the layer and substrate according to the formula

$$\Delta a_{\Delta T} = -(\alpha_L - \alpha_s)\Delta T\, a_0 \frac{2\nu}{1-\nu} \tag{5}$$

α_L, and α_s are the coefficients of thermal expansion of the layer and substrate respectively, a_0 is the lattice parameter of stoichiometric TiN, $\nu = 0.2$ is the Poisson constant and ΔT is the temperature difference before and after the reaction.

The resulting lattice parameters for compact layers on the substrate are shown in Fig. 10. In all cases their values range above the tabulated value $a_{TiN} = 0.4240$ nm and they increase remarkably with the bias. The value of the lattice parameter also varies with the nitrogen flow rate, its maximum being attained in the range for maximum microhardness values.

The lattice parameters were also caclulated for TiN_x layers after their separation. These coatings are no longer textured and thus the resulting lattice parameter was calculated for them as the arithmetic mean value of lattice parameters for the (111), (200) and (220) planes. The values of these lattice parameters are decidedly lower and range near the value $a_{TiN} = 0.4240$ nm given in standard tables. The resulting values are shown in Fig. 11.

Figure 12 shows the difference between lattice parameters of the layer before and after separation *vs.* the nitrogen flow rate. The dependence follows a similar course to that in Fig. 10; however, the maxima in the region of the highest microhardness values are significantly sharper.

From the graphs presented it can be concluded that high values of the lattice parameters of compact TiN_x layers result in particular from high values of the macroscopic stress produced in the layer in the course of the deposition. This stress results mostly from the action of the bias in combination with the ion current and not from the difference in the thermal expansions of the layer and substrate.

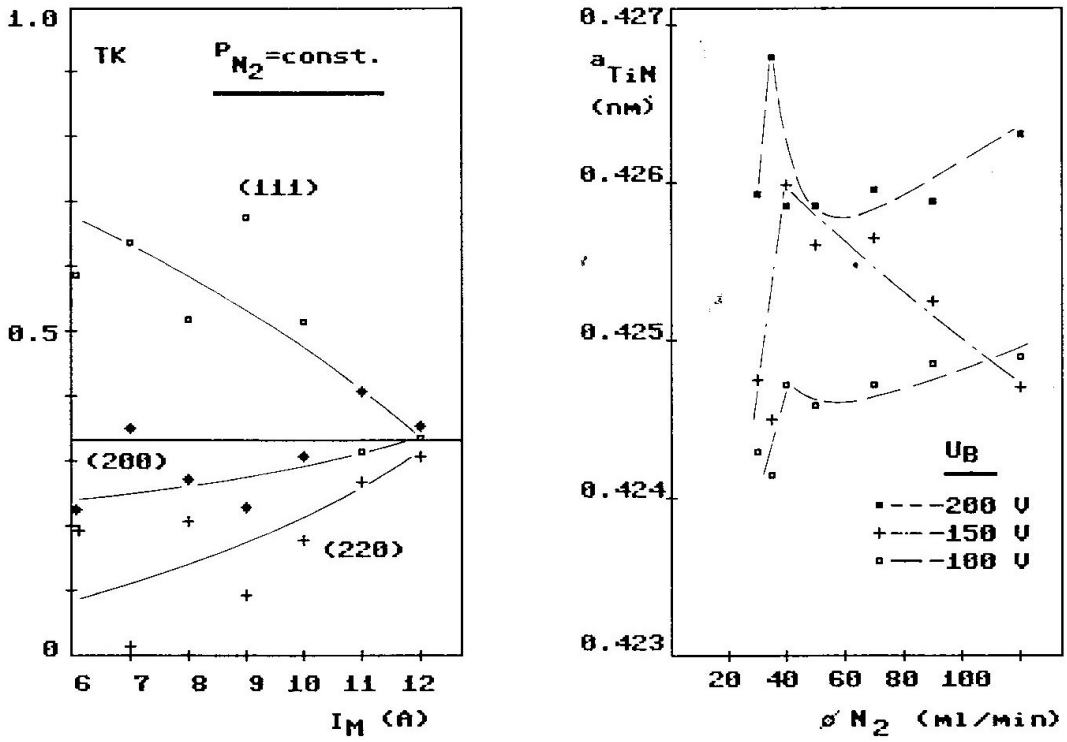

Fig. 9. The dependence of the texture on the current at the PK 500 cathodes.

Fig. 10. The dependence of the lattice parameters on the nitrogen flow rate for compact TiN_x layers deposited at $U_B = -100, -150$ and -200 V.

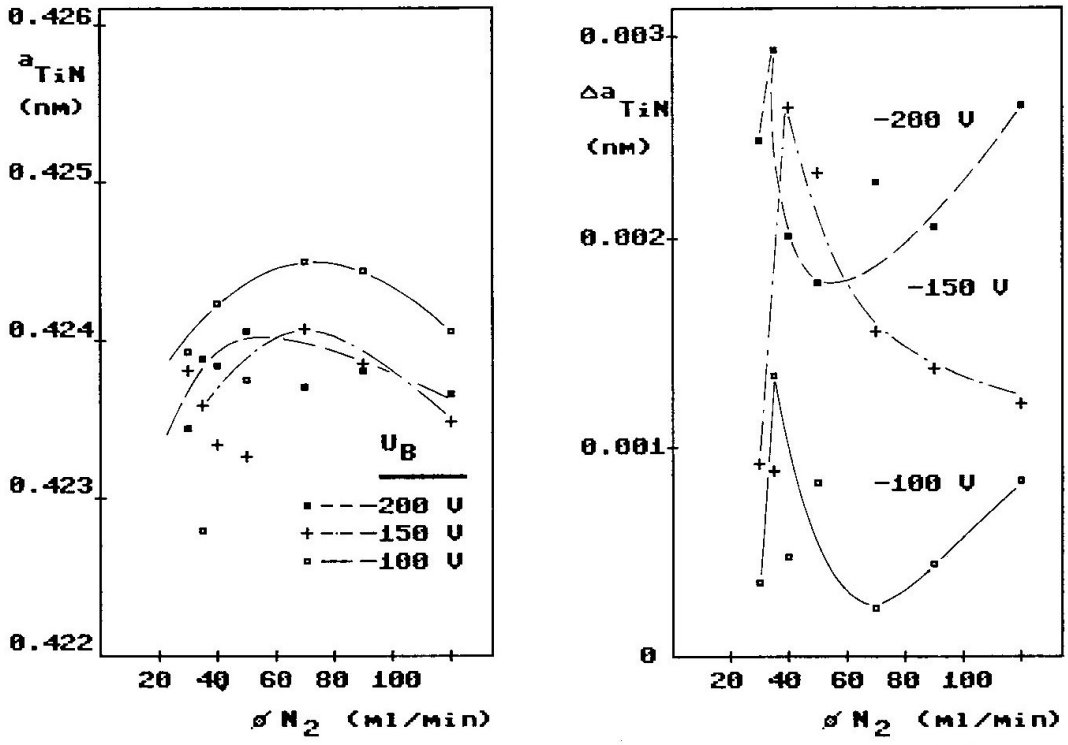

Fig. 11. The dependence of the lattice parameters of TiN_x on the nitrogen flow rate for layers separated from the substrate.

Fig. 12. The difference between values of the lattice parameters of compact TiN_x layers and separated layers as a function of the nitrogen flow rate.

4.6.3. Macroscopic stresses

In the case of known values of the lattice parameters of TiN_x layers before and after separation, it is possible to calculate the magnitude of the macroscopic stresses in the layer according to the following formula:

$$\sigma_1 + \sigma_2 = \frac{E}{\nu} \frac{\Delta a}{a_0} (\text{MPa}) \tag{6}$$

where E (MPa) is the modulus of elasticity in tension for TiN. This stress is prevalently of a compressive character and under certain conditions it achieves extreme values of $(5\text{–}6) \times 10^3$ MPa.

Figure 13 shows the dependence of Δa_{TiN} on the bias as a mean value of this change for several sample series. The dependence indicates that in a region $U_B < -60$ V there are tensile stresses in the layer, which are changed to compressive stresses with increasing bias value. Maximum values of the compressive stresses are achieved at $U_B = -200$ to -250 V. The value of these stresses is even below the level of the cohesion strength of the basic material. When suitable deposition parameters are chosen, it is, in contrast with this, possible to deposit TiN_x layers without any internal stress.

The magnitude of the internal stress and the layer texture are associated with each other in a region of superstoichiometric values of x. Figure 14 shows the dependence of TK_{111} on the substrate bias for two series of samples, which complemented those used for following the effect of the partial pressure. The films were deposited at a constant nitrogen flow rate (50 ml N_2 min^{-1}) with a stepwise increasing bias $U_B = 0, -30, -65, -100, -150, -200, -250$ and -300 V. One series was produced at an argon flow rate of 200 ml min^{-1} ($p_T = 1.1$ Pa), the second series at 150 ml Ar min^{-1} ($p_T = 0.8$ Pa). The graph demonstrates that higher values of U_B support the growth of crystallites with the orientation (111) and maximum degree of texture above $U_B = -200$ V. This region corresponds to the region of maximum values of the microscopic stresses. The lower U_B value decreases the proportion of crystallites with the orientation (111) and increases those with (200) and (220) orientations.

The magnitude of the macroscopic stresses is also affected by the value of the ion current i (mA cm^{-2}) on the substrate.

In Fig. 15 values of the lattice parameters of layers before and after separation are plotted for a series of samples where the current density was varied as a basic parameter by changing the magnetron power. With increasing current value the difference between the lattice parameters of the compact layer and the separated layer distinctly decreases. Thus, the internal stress decreases in the layer in the same way as its (111) texture according to Fig. 9.

4.6.4. The microscopic stresses

Some microscopic stress remains in the layer even after separation of the layer from the substrate. This is an internal elastic stress, which is balanced over a region of several grains. The magnitude of the microstress may be established from the broadening of the (111), (200) and (220) diffraction lines of TiN after subtracting the effect of diffraction line widening due to coherent scattering and density dislocations. The resulting values are presented in Fig. 16 for all three series of samples. The

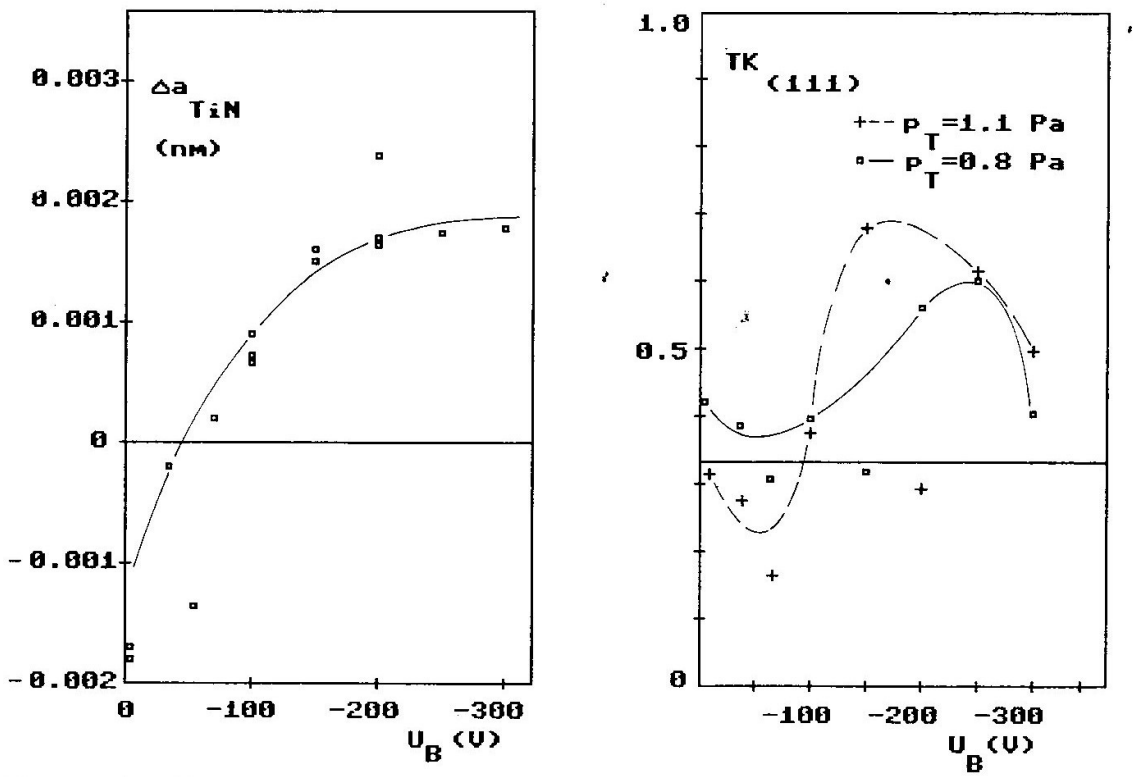

Fig. 13. The difference between values of the lattice parameters of compact TiN_x layers and separated layers as a function of the bias.

Fig. 14. The dependence of TK_{111} on the bias U_B for different magnitudes of the total pressure during deposition.

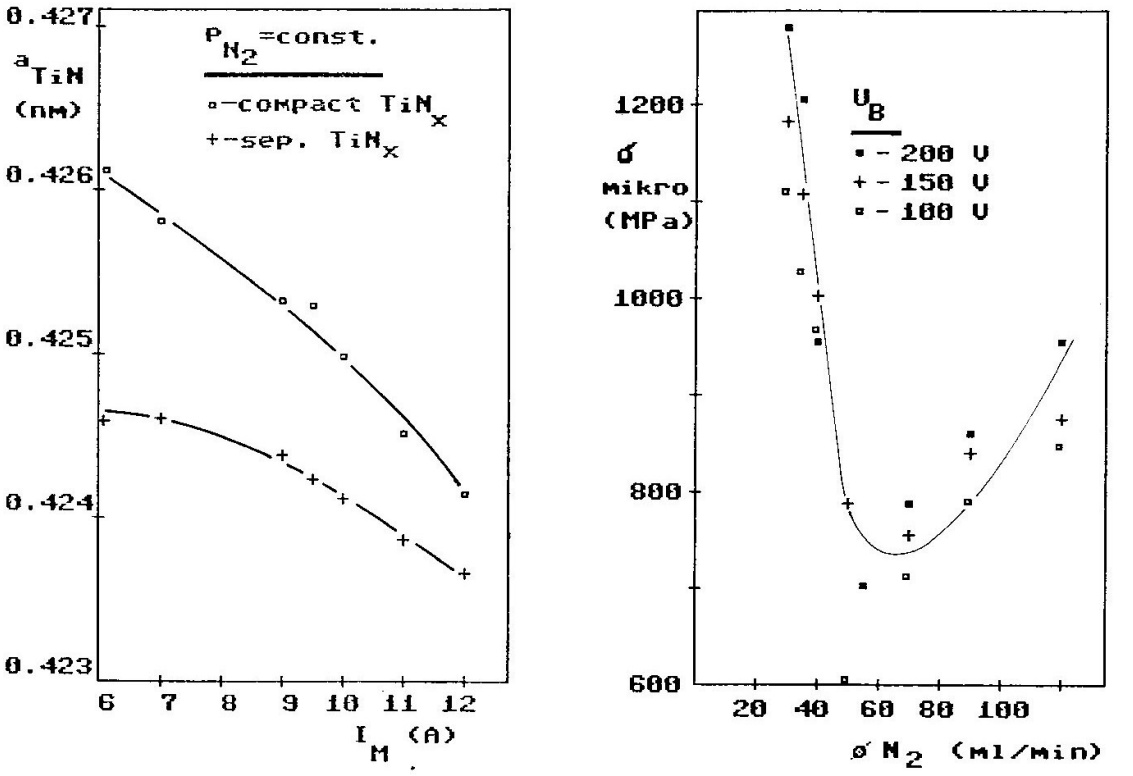

Fig. 15. The dependence of the value of the lattice parameter on the magnetron power for compact and separated TiN_x layers.

Fig. 16. The dependence of the value of the microscopic stress on the nitrogen flow rate.

microstress exhibits a marked minimum at a nitrogen flow rate of 50 ml min^{-1}. This minimum corresponds approximately to minimum values of the macrostresses according to Fig. 12.

4.6.5. The chemical composition of TiN_x layers

On the basis of the lattice parameters determined for the separated coatings, it is possible to evaluate the chemical composition of TiN layers, *i.e.* their stoichiometric ratio N:Ti. For the correction of lattice parameters of separated layers for the stress originating from the different thermal expansivities of the layer and substrate, we obtain values of the lattice parameters, expressing the chemical composition. The theoretical dependence was established on the basis of data from the literature[7,9,10,11] and is shown in Fig. 17.

The following formulae may be employed: for substoichiometric layers,

$$x_N = \frac{\langle a \rangle_{\Delta T,TK} - 4.2128}{0.056} + 0.5 \tag{7}$$

and for superstoichiometric layers,

$$x_N = -\frac{\langle a \rangle_{\Delta T,TK} - 4.2460}{0.230} + 1.0 \tag{8}$$

The resulting values of the chemical composition which were determined from the magnitudes of the lattice parameters are shown in Fig. 18 and they correspond to results in Figs. 5 and 6. The values of the stoichiometric ratio are strongly affected by

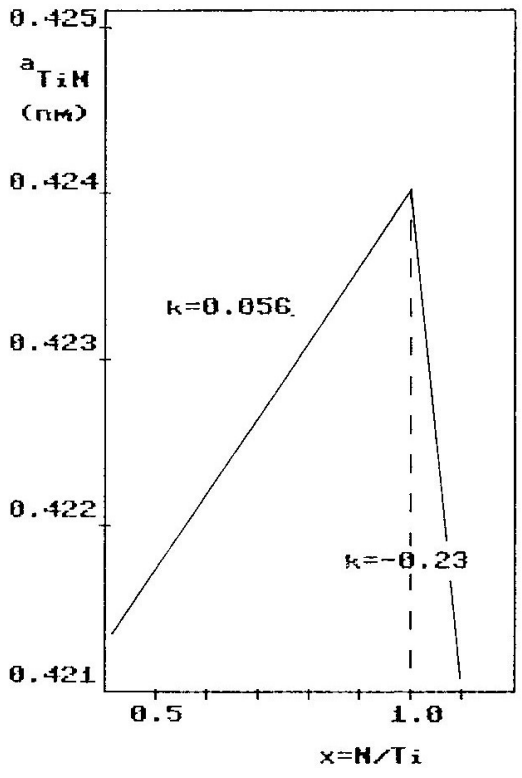

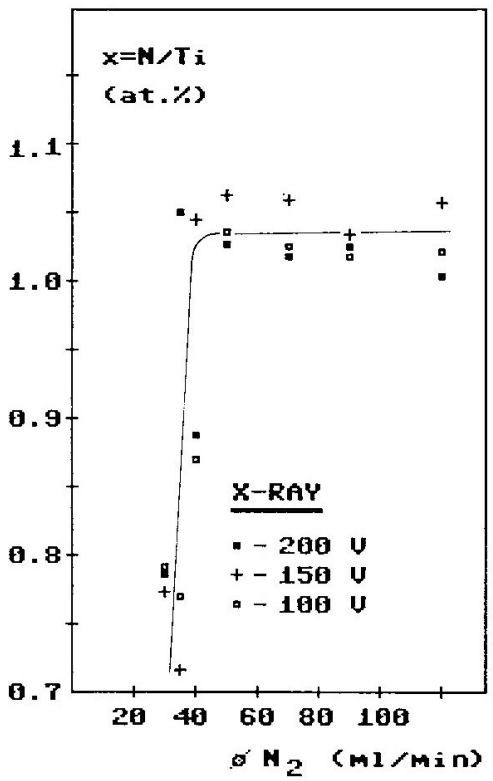

Fig. 17. The theoretical dependence of the value of the lattice parameter of TiN_x on the stoichiometric ratio x.

Fig. 18. The dependence of the N:Ti stoichiometric ratio on the nitrogen flow rate for series at $U_B = -100$, -150 and -200 V evaluated by X-ray diffraction.

the flow rate up to 40 ml N_2 min^{-1}, whereas above this value the changes in the layer's chemical composition are only small.

The effect of the bias on the change in the layer's chemical composition is not distinct. In spite of this fact, in a series of samples which were prepared at a constant value of the nitrogen flow rate of 50 ml min^{-1} with stepwise increases in the bias, there was a stepwise increase in the lattice parameter in separated coatings. These layers no longer have a macroscopic stress and therefore this fact may be explained only by a change in the layer's chemical composition, *i.e.* by a reduction in vacancies at titanium sites of the lattice.

4.7. The colour of TiN_x layers

Figure 19 shows the colour coordinates of TiN_x layers as a function of the nitrogen flow rate for a bias $U_B = -150$ V. With increasing nitrogen flow rate the coordinates a^* (red) and b^* (yellow) are stepwise increased. A steep increase in these values starts at a flow rate of 35 ml min^{-1}, *i.e.* in the region at which the stoichiometric N:Ti ratio is attained. With a further increase in the nitrogen flow rate, the portion of the red colour in particular increases, and the colour of the layers becomes reddish brown.

The dependence of colour coordinates on the bias U_B is plotted in Fig. 20. From the dependence it is obvious that the bias increases the proportion of the yellow colour in the layer; the layers gain a golden tint. The amount of red remains nearly constant.

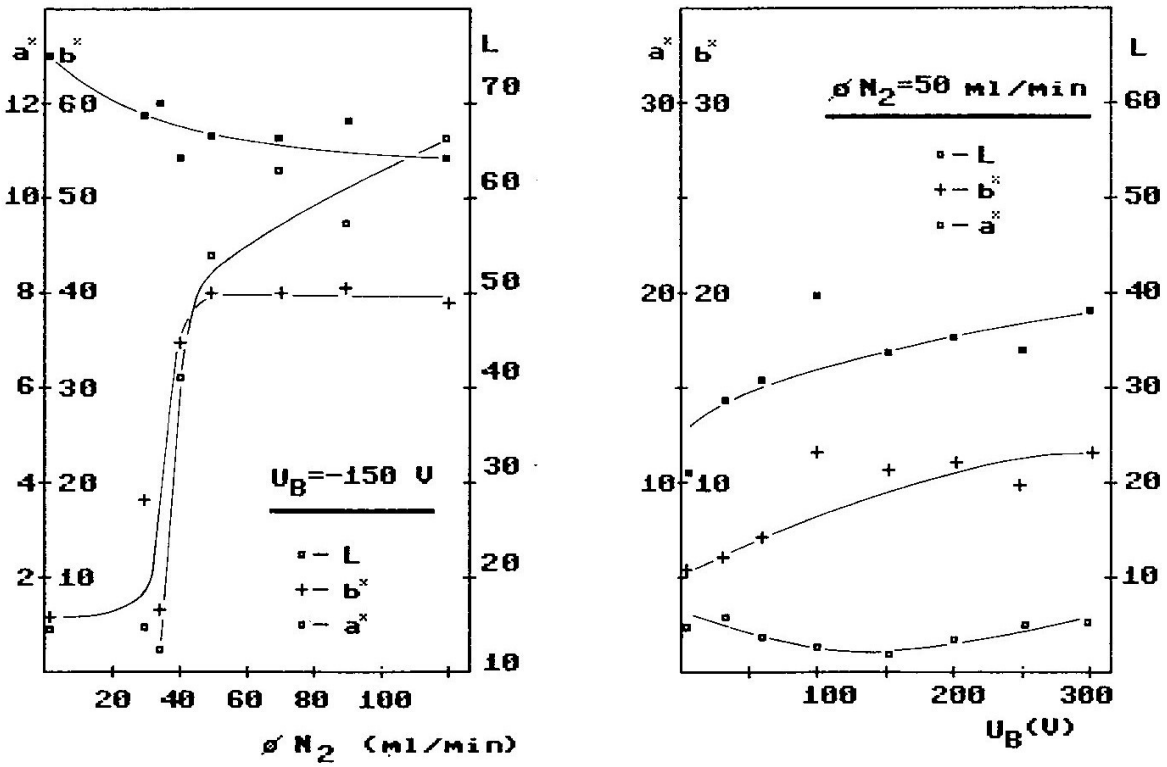

Fig. 19. The dependence of the values of the CIEL colour coordinates a^*b^* for TiN_x layers on the nitrogen flow rate for $U_B = -150$ V.

Fig. 20. The dependence of the values of the CIEL colour coordinates a^*b^* on the bias value for a series of samples with a nitrogen flow rate of 50 ml min^{-1}.

From the measured colour coordinates it follows that the change in the colour quality of TiN_x layers is a parameter which is very sensitive to their characteristics, particularly to the chemical composition. The increase in the proportion of the yellow colour with increasing bias indicates almost unambiguously a decrease in the values of x for superstoichiometric coatings.

4.8. The wear tests

During the evaluation of the characteristics of TiN_x layers to be used for cutting tools, their resistance to wear is of decisive importance. Thus, in all the dependences, for $U_B = -100$, -150 and -200 V, cutting tests were performed with 6 mm drills. Conditions were used for which the time of testing was the minimum possible to obtain a sufficient set of data.

The result of the test for layers deposited at $U_B = -150$ V as a function of the nitrogen flow rate is shown in Fig. 21. The tool with a layer of pure titanium has a drilling edge of almost zero durability. With increasing nitrogen flow rate, the tool durability increases stepwise, and achieves its maximum at a flow rate of 50 ml min^{-1}. The maximum number of holes obtained by drilling is about 120; this number is not significantly altered by further increases in the nitrogen flow rate. A very similar dependence was also achieved for $U_B = -100$ and -200 V. The maximum values of the number of holes obtained by drilling were also the same.

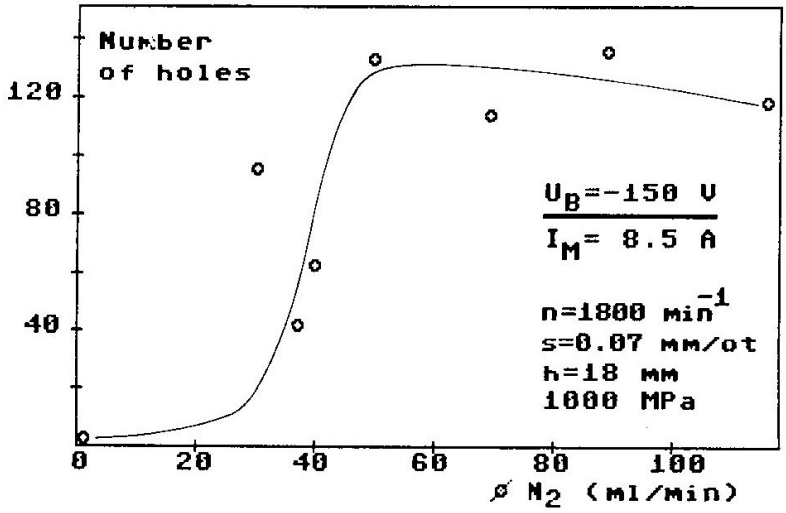

Fig. 21. The evaluation of the durability of 6 mm diameter drills for a series of samples with $U_B = -150$ V at $s = 0.07$ mm $round^{-1}$.

Figure 22 presents a similar dependence for the same series of samples, but with a shift $s = 0.14$ mm rev^{-1}. Thus the drilling conditions were even more exacting. In this case, the dependence also exhibits a marked maximum, which again is present at a flow rate of 50 ml min^{-1}. When the resulting values are inserted into the Taylor relationship

$$v_s = C_s T^{-1/k} \tag{9}$$

(where v_s is the shift velocity, T is the tool durability, k is the slope of the straight regression line in a logarithmic coordinate system and C_s is the shift velocity for unit durability of the drilling edge), the optimum parameters of the layer are obtained for

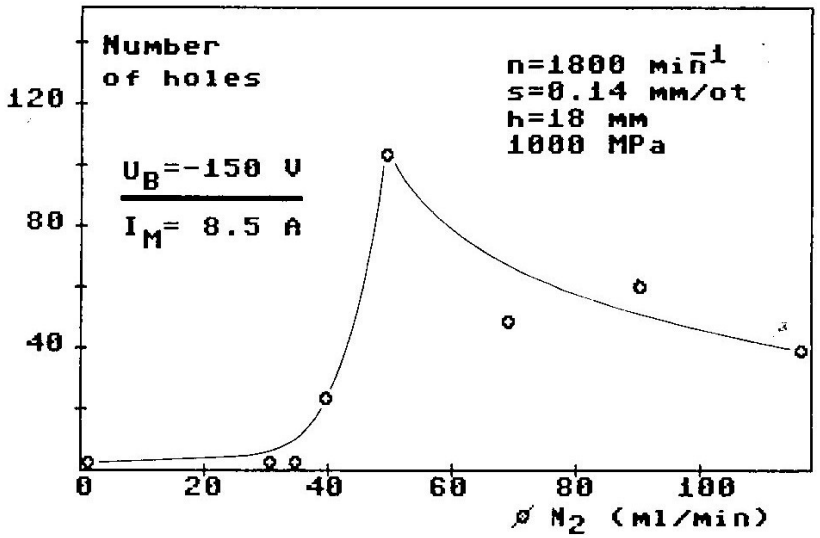

Fig. 22. The evaluation of the durability of 6 mm diameter drills for a series of samples with $U_B = -150$ V at $s = 0.14$ mm round^{-1}.

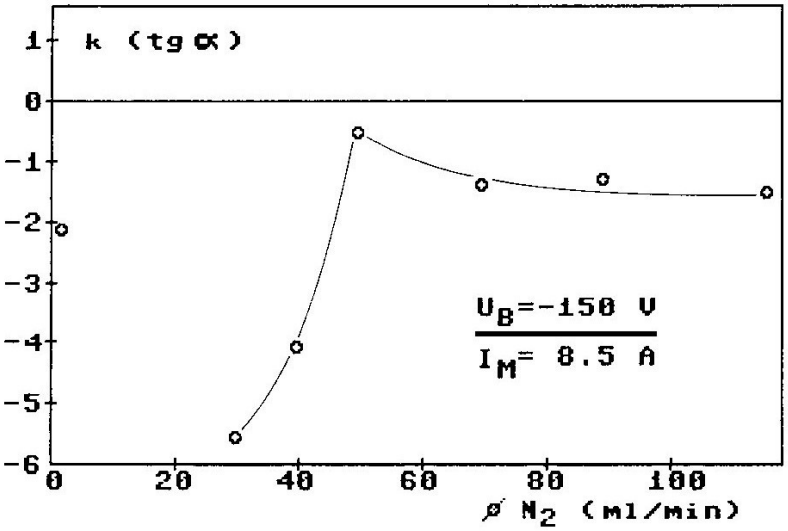

Fig. 23. Calculated values of the slope of the straight regression line in the T–v diagram for different nitrogen flow rates.

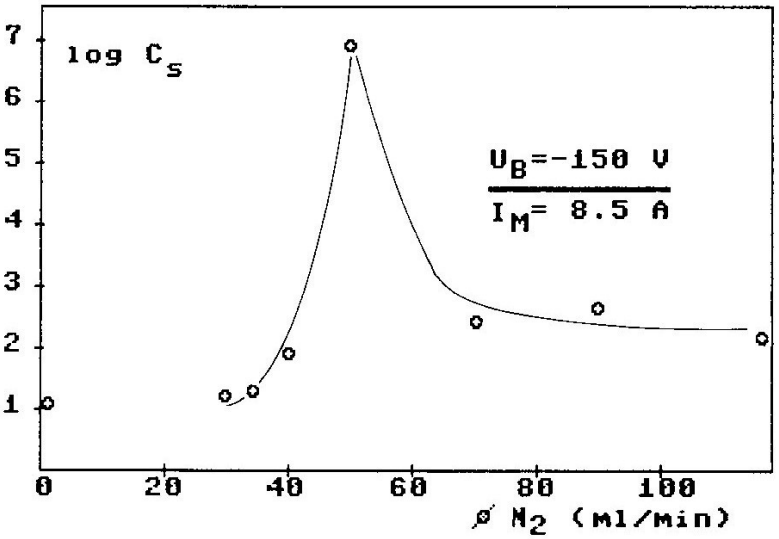

Fig. 24. Calculated values of C_s in the T–v diagram as a function of the nitrogen flow rate for $U_B = -150$ V.

a straight regression line having the smallest slope and for a C_s value on the x axis attaining a maximum. The dependences of these values on nitrogen flow rate are presented in Figs. 23 and 24. A minimum slope of the straight regression line at a maximum C_s value was achieved for a nitrogen flow rate of 50 ml min^{-1}.

This means that the highest durability of the layer against wear is found in this region, together with a simultaneously occurring highest oxidation stability.

At a shift $s = 0.07$ mm round^{-1} there was no significant effect of the bias on the cutting quality of the 6 mm drills. At a shift of 0.14 mm rev^{-1} markedly better values of T were, however, obtained at a bias of $U_B = -150$ V compared with those at $U_B = -200$ V.

5. DISCUSSION

The results in the preceding section indicate that the problems arising in the deposition of the TiN layers are very complicated. Certain deposition parameters affect the TiN_x properties strongly and a thorough understanding of the deposition process is necessary to obtain optimum characteristics of the TiN_x layers.

From the standpoint of useful characteristics of TiN_x, the effects of the bias on the substrate and of the nitrogen partial pressure in particular were investigated. The strong dependence of the TiN_x layer's chemical composition on the partial pressure is specific for magnetron deposition and it is explained by a lower percentage of ionized particles in the plasma. Thus only a minor portion of nitrogen is bound chemically during layer condensation and most of it is bound physically. The optimum value of the partial pressure has to be chosen in such a way that layer deposition occurs with a maximum rate; however, the stoichiometric ratio N:Ti of the layer should be in a region with $x > 1$. In this region the useful characteristics of TiN_x are, however, governed in particular by the physical parameters of the layer, *i.e.* the structure and morphology, macroscopic and microscopic stresses and layer texture. These parameters are affected in a decisive manner by the deposition temperature, the value of the bias and the ion current density on the substrate.

When it is attempting to achieve maximum useful parameters of the layer then, according to the results of cutting tests, these values are attained in a region of the nitrogen flow rate for which the maximum (111) layer texture is exhibited and where minimum macroscopic and microscopic stresses exist in the layers. Maximum values of the layer adhesivity to the substrate are also found in this region.

The bias on the substrate is a decisive parameter generating the stress in the layer. A certain minimum value of U_B is necessary for optimum growth of the layer and for its purity. However, in practice its value is selected in a way which allows thermal equilibrium on the substrate to be achieved, *i.e.* with respect to the ion current density. In the case of a low particle current density from the source it is necessary to have a high bias, and vice versa. However, the high bias results in high values of the internal stress, which is undesirable for the adhesivity of the layer as well as for its mechanical characteristics. Thus the purpose is to increase the ion current value, *e.g.* by the power at the cathode, in such a way that the value of U_B can be below -100 V. That value of U_B is ideal; the internal stress in the layer achieves zero or minimum values.

6. CONCLUSION

In spite of the remarkable extent of experimental work aimed at elucidating the effect of certain deposition parameters on important characteristics of TiN_x, a number of phenomena still remain unclear. It is concluded that the magnetron deposition of TiN_x layers is a potentially useful approach. The main step in the further development of this deposition method lies in increasing the ionization in the space between the cathode and substrate with the aim of increasing the density of the ion current on the substrate.

ACKNOWLEDGMENTS

The authors are indebted to Dr. Sundgren (University of Linköping) for facilitating the Auger analysis and to Dr. Munz (Leybold AG) for supplying experimental material for cutting tests.

REFERENCES

1 A. F. Hmiel, *J. Vac. Sci. Technol. A, 3* (3) (1985) 592–595.
2 S. Kadlec, *Vacuum, 10* (1987) 729–738.
3 U. Helmersson, *J. Vac. Sci. Technol. A, 3* (2) (1985) 310–314.
4 L. Hultman, *Thin Solid films, 124* (1985) 163–170.
5 V. Poulek, *Res. Rep. 49/88*, May 1988 (CSAV, Prague).
6 J. Sundgren, *J. Vac. Sci. Technol A, 4* (5) (1986) 2259.
7 J. Sundgren, *Thin Solid Films, 105* (1983) 353–366.
8 P. T. Dawson and K. K. Tzatzov, *Surf. Sci., 194* (1985) 105.
9 E. Bumps, *Trans. ASM., 45* (1953) 1008.
10 B. Holmberg, *Acta Chem. Scand., 16* (1962) 1262.
11 L. Toth, *Transition Metal Carbides and Nitrides*, Academic Press, New York, 1971.